

# PhotonAssay™: A Review of Real-World Performance on Heterogeneous Gold Ores

*J Tickner<sup>1</sup>, Joel Chuah, Andrew Weatherstone and Tim Sennett*

Chrysos Corporation Ltd, Australia

<sup>1</sup> Corresponding author: email james.tickner@chrysoscorp.com

## Abstract

PhotonAssay™ is a non-destructive gold assay method based on gamma activation analysis which has been applied extensively across a wide range of gold ore types. This paper reviews real-world performance on heterogeneous ores, with emphasis on method comparison, sampling behaviour, and the practical significance of positional heterogeneity. The underlying physics of PhotonAssay™ allows direct measurements on aliquot masses typically an order of magnitude larger than conventional fire assay. Results from certified reference materials, large-scale feasibility studies, and detailed case studies across multiple deposit styles are examined. Across these studies, PhotonAssay™ shows strong agreement with fire assay and measurements on coarse and pulverized materials are consistent, with mean grade ratios generally close to unity and high correlations observed across diverse geological settings. The findings indicate that larger assay masses can reduce total sampling variance relative to conventional small-charge fire assay, particularly in coarse or nuggety ores where sub-sampling error dominates. Although spatial sensitivity variations within the sample jar are physically real, theoretical analysis and empirical evidence show that their contribution to total uncertainty is modest in practical applications. Overall, PhotonAssay™ provides a technically robust and operationally advantageous alternative for gold analysis on heterogeneous ores.

## 1. Introduction

The accurate determination of gold grade in mineral ores remains one of the most technically challenging analytical problems in the mining industry. Gold is commonly present at concentrations of only a few parts-per-million or below, is frequently distributed extremely heterogeneously, and often occurs in forms that create substantial sampling variance during conventional analytical workflows. Traditional analytical approaches, notably fire assay [1], have consequently evolved around extensive particle-size reduction and careful sub-sampling protocols intended to minimise these sampling effects.

Gamma activation analysis (GAA) [2-5] has been explored as an alternative method for gold assay since the early 1960s. Rather than chemically extracting gold from a small, pulverised aliquot, the technique directly measures gold atoms within a comparatively large sample using high-energy X-rays and subsequent detection of characteristic gamma-ray emissions from activated nuclei.

Chrysos' PhotonAssay™ provides the first widely available implementation of GAA and has been in commercial use since 2018. The physical principles underpinning the method have been extensively described elsewhere [6]. Samples are activated using high-energy X-rays to excite the naturally occurring gold isotope Au-197 into a short-lived isomeric state which subsequently decays via emission of a characteristic 279 keV gamma-ray. The high penetration depths of both the incident X-rays and emitted gamma-rays permit bulk analysis of samples weighing several hundred grams.

A key consequence of this physics is that the measurement process is fundamentally insensitive to the chemical form of the gold and substantially insensitive to the physical presentation of the sample. Unlike chemical extraction methods, the PhotonAssay™ process does not rely on dissolution, melting, liberation or exposure of gold particles at freshly fractured surfaces. Instead, the main factors affecting analytical performance are the statistical uncertainty associated with counting the characteristic gamma-rays, and the accuracy of the corrections applied for gamma-ray attenuation and detection efficiency.

When considering the performance of any assay method, it is important to distinguish between genuine analytical performance (precision, accuracy and bias) and important but distinct factors relating to sampling. In short: how well does a method perform on the material with which it is presented, versus is that material representative of the original bulk?

The performance of PhotonAssay™ can be approached both empirically and theoretically.

Published [7-10] and extensive unpublished empirical studies have now been conducted on PhotonAssay™ performance using certified reference materials, drill core, reverse circulation samples, coarse rejects, process pulps and highly nuggety ores from a wide range of deposit types and geological domains.

Collectively, these studies comprise several hundred thousand comparison analyses and have been used to explore whether:

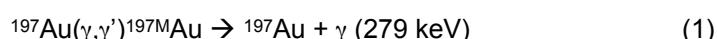
- any systematic normalisation (bias) differences are observed between crushed and pulverised samples, or between PhotonAssay™ and fire-assay measurements
- sampling behaviour follows well-established Theory of Sampling principles, namely decreasing with increasing sample mass and with reduced particle size
- the larger sample masses used in PhotonAssay™ reduce total sampling variance relative to conventional small-charge fire assay, even when performed without pulverisation
- observed positional or particle-size effects are important in practical operational contexts when appropriate preparation protocols are employed.

The present paper provides a technical evaluation of these issues, with particular emphasis on the comparison methodology, interpretation of sampling effects, and the practical significance of positional heterogeneity. Empirical findings are presented with supporting theoretical reasoning and modelling.

## 2. Physics of PhotonAssay™ Measurement

PhotonAssay™ is based on gamma activation analysis using high-energy X-rays generated by an electron linear accelerator. The accelerator is an electronic source that only produces X-rays when energised. For gold analysis it is operated to produce an X-ray beam with energies up to 8.5 MeV; for comparison, a method such as portable X-ray fluorescence (pXRF) uses a source operating at much lower energies of around 50 keV (0.05 MeV).

The reaction used for gold analysis is:



Gold comprises 100% of the only naturally occurring isotope Au-197. A gold nucleus absorbs a high-energy X-ray, converting it to a short-lived excited or meta-state. This state has a half-life of 7.73 seconds and decays to usually (70.9% probability) produce a gamma-ray with a distinctive energy of 279 keV [11].

A PhotonAssay™ measurement (Figure 1) consists of a 15 s period of sample irradiation during which the gold activity builds up, followed by a 15 s period of measurement during which the emitted 279 keV gamma-rays are detected and counted. Samples are automatically transferred between irradiation and measurement locations using a robotic shuttle. Each sample is typically measured for two irradiation/measurement cycles to improve sensitivity.

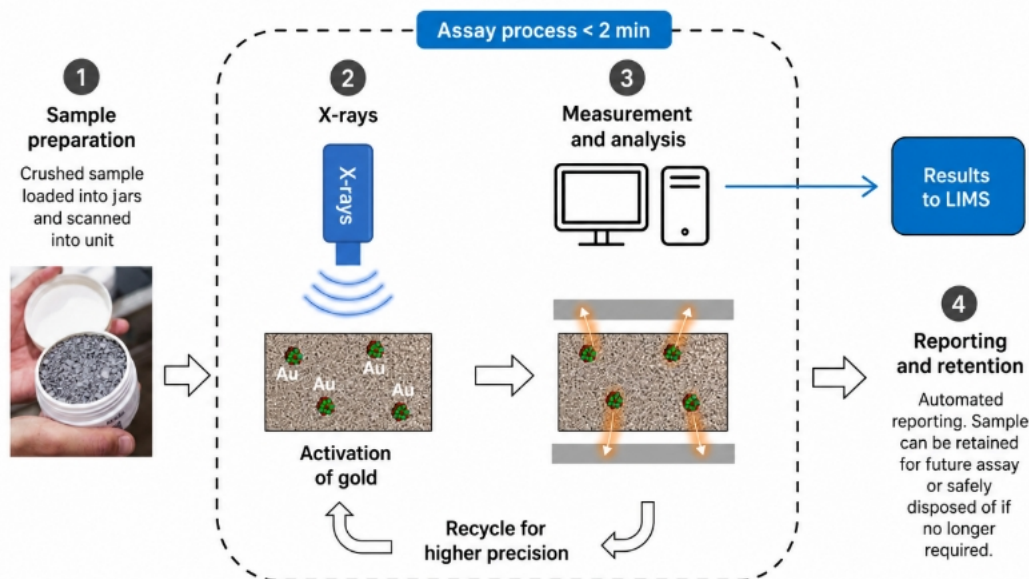


**Figure 1. The PhotonAssay™ workflow: (1) samples are loaded into jars and registered (2) samples are irradiated using high-energy X-rays for 15 s to activate gold (3) samples are then transferred to a measurement station and gamma-rays counted using twin detectors; process repeated and results averaged (4) grades automatically calculated and reported.**

An important design goal is to optimise analytical performance by balancing three competing aims:

- maximise the sample volume (and hence sample mass) to reduce the Fundamental Sampling Error [12]
- maximise sensitivity for low gold grades by placing the X-ray source and gamma-ray detectors close to the sample
- minimise sensitivity to the location of gold within the sample volume to ensure a 'flat' system response.

The optimal design uses cylindrical sample jars approximately 100 mm in diameter and 50 mm high; these have a volume of 320 mL and typically hold 400-600 g of crushed ore or 300-500 g of pulverised ore. Samples are irradiated and measured with their axis oriented vertically (lid uppermost). Irradiation is performed through the side wall of the jar with the sample continuously rotating. Samples are measured between two cylindrical detectors (90 mm diameter) positioned immediately above their top and bottom surfaces.

This configuration allows analysis of a sample mass typically 10 times that of conventional fire-assay and affords a detection limit of 0.01 ppm. Variations in sensitivity of gold detection throughout the sample volume are discussed below.

A reference disc containing a bromide salt is placed in a pocket at the base of the sample jar and irradiated and measured alongside each sample. Bromine has a similar activation reaction to gold but produces a distinct and lower energy gamma-ray (207 keV). The bromine signal provides an automatic correction for any variations in the output of the X-ray source or detector efficiency.

The penetration of X-rays and gamma-rays through solid material is described in terms of the mean-free path (MFP), which is the average distance travelled before interaction or absorption. The MFP depends on material density, but at the energies involved in PhotonAssay™ is only a very weak function of composition for typical rock matrices. For a common crushed-ore density of 1.6 gcm<sup>-3</sup>, the MFP exceeds 200 mm for the incident high-energy X-rays and is 50-60 mm for the 279 keV gold gamma-rays. As these values are much larger than the top particle size in even coarse-crushed samples, the analysis is effectively

insensitive to particle size. Of course, particle size affects the Fundamental Sampling Error, a point discussed in more detail later.

As the MFP values for the incident X-rays and emitted gamma-rays are comparable to the jar dimensions, determining the gold grade from the gold signal (measured 279 keV gamma-ray intensity) requires a correction for X-ray and gamma-ray attenuation inside the sample and a geometry correction for where the sample material is located with respect to the top and bottom detectors. These corrections are determined using the measured mass and sample fill levels that are recorded when the jar is scanned into a PhotonAssay™ system. A factory-set look-up table returns the appropriate correction factor from supplied mass and fill values.

Substantial experimental work has validated – in line with the theoretical arguments presented - that PhotonAssay™ is substantially insensitive to sample matrix and physical form across a wide range of ore types and process materials. A summary of this work is presented below, and more details are available in a range of Chryso technical notes [10,13-14]. This behaviour contrasts fundamentally with conventional chemical assays, where liberation, dissolution kinetics, flux behaviour, reagent chemistry, and aliquot representativity all influence the final reported grade.

### **3. Method Comparison Framework**

Comparison of different assay methods for gold ores is statistically non-trivial. Ore grade distributions are typically strongly skewed, heteroscedastic, and frequently dominated by sampling variance rather than instrumental precision. Naïve application of methods such as linear regression, ANOVA, correlation coefficients, or conventional Bland–Altman plots can produce misleading conclusions when applied to mineral assay data.

Meaningful comparison requires explicit consideration of sampling variance, grade distribution shape, multiplicative rather than additive error structures, aliquot independence, and the contribution of both preparation and analytical errors.

The framework adopted here follows the methodology developed in previous work [15] comparing PhotonAssay™ and fire assay results on large ore suites. We consider the following principles to be particularly important:

#### **(a) All assay methods return an approximation to “truth”**

In real ore materials, all methods measure aliquots drawn from larger heterogeneous masses. Consequently, disagreement between two assays does not necessarily imply analytical bias, and observed scatter frequently reflects sampling effects rather than instrumental failure. For chemical methods, recoveries of the analyte from the ore matrix may be less than 100%, and all methods are subject to both random and systematic normalisation errors.

#### **(b) Sampling effects dominate in coarse gold ores**

For coarse gold ores, differences between two assays performed on different aliquots may substantially exceed instrumental uncertainties. Where coarse gold or nugget effects are present, larger assay masses generally improve representativity.

#### **(c) Statistical equivalence is more important than pointwise agreement**

For operational applications such as resource definition, grade control and reconciliation, the critical question is whether two methods produce statistically interchangeable grade populations. Measurement and sampling uncertainties make pointwise comparison less useful than population level metrics.

Following [15], our primary tool for assessing overall bias between different assays performed on the same sample suite is the logarithmic Tukey ratio plot. In such a plot (Figure 2, right) the pairwise ratio of grade measurements obtained using two different methods (y-axis, logarithmic scale) is plotted against the geometric mean grade (square-root of the product of the two grade measurements, x-axis, logarithmic scale).

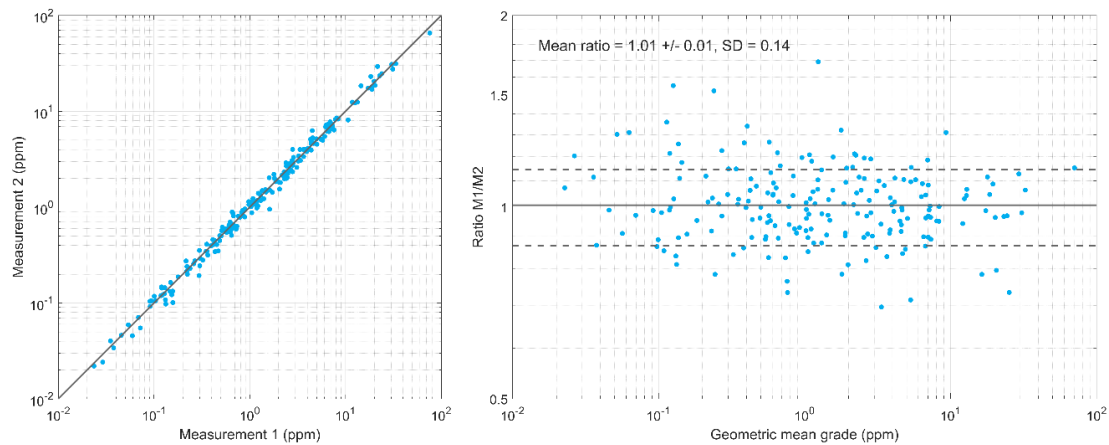


**Figure 2. Traditional scatter plot on logarithmic axes (left) and Tukey ratio plot (right) for a synthetic data set comprising 200 samples with log-normal grade distribution. For each sample, grades are modelled assuming two independent, unbiased measurement methods each with a precision (relative SD) of 10%.**

By focussing on the *differences* in the ratio of measured values from unity, the Tukey plot provides a much more sensitive illustration of small biases than a traditional scatter plot (Figure 2, left). Data cleaning – removal of obvious sample swaps, transcription errors, values below detection limit on one or both methods – is also facilitated. Finally, subtle *trends* in bias versus grade, often indicative of contamination during preparation, are also made readily apparent.

Any overall bias and its experimental uncertainty can be readily determined following the procedures detailed in [15]. The example illustrated in Figure 2 is based on a synthetic data set comprising 200 samples with a log-normal grade distribution. For each sample, grades are assumed to be measured by two independent, unbiased methods with a precision (relative SD) of 10%. The resulting mean ratio (1.01 +/- 0.01) is statistically consistent with unity and the RSD on the pairwise ratio of measured grades (0.14) is consistent with the 10% contributions from each measurement, added in quadrature.

While the Tukey ratio plot is the preferred visual diagnostic for the reasons set out above, a range of statistical tests can also be used to characterise method agreement. A one-sample, two-tailed t-test on the log-transformed pairwise ratio is used to test the null hypothesis that the mean log ratio is zero, or equivalently that the two methods are unbiased relative to one another. The log transformation is appropriate given the multiplicative error structure and log-normal grade distributions typical of gold deposits and yields a test statistic whose assumptions - approximate normality and homoscedasticity - are better satisfied than for tests performed on the raw grade differences.

In parallel to the t-test, Cohen's d effect size is used as a standardised measure of effect size. The t-test addresses whether any difference observed between methods is distinguishable from zero with the given data. Conversely, Cohen's d effect size quantifies the magnitude of the difference and addresses the question of whether it is material. Conventional thresholds ( $|d| < 0.2$  small, 0.2–0.5 medium,  $> 0.5$  large) provide guidance on the effect size and do not collapse with increasing sample size.

This is an important distinction, as statistical significance under hypothesis testing is not the same as practical significance. With a sufficiently large sample size, a t-test (or any hypothesis test) will reliably reject the null hypothesis of zero bias for arbitrarily small mean log ratios — differences that are immaterial for resource definition, grade control or reconciliation. Conversely, a small study may fail to reject the null hypothesis for a bias that would matter operationally. Collectively reporting the Tukey mean ratio, t-test and Cohen's d effect size allows the user to separate out “detectable” difference from a “meaningful” difference.

## 4. Prior Experimental Studies

### 4.1. Certified Reference Materials

Initial validation of PhotonAssay™ was performed using suites of certified reference materials (CRMs) spanning multiple ore matrices, wide grade ranges, and provided by numerous manufacturers. The most comprehensive of these studies is reported in Chrysos Technical Note TN-001 [13], which documents CRM test work conducted over the period 2019–2022 across multiple deployed PhotonAssay™ units in Western Australia.

Figure 3 presents results from the combined manufacturer study (suite S4 in TN-001), which included 94 CRMs sourced from CDN, OREAS, Rocklabs and Geostats and measured using PhotonAssay™. The CRM suite included a broad range of ore types, including sulphides, gold/copper ores, concentrates and oxides, and each CRM was measured using at least a 6 × 2 cycle analysis. The certified grades of these CRMs spanned several orders of magnitude (0.1–87 ppm). The reported  $R^2$  between PhotonAssay™ and the certified values is 0.99994, as shown in Figure 3 (top). Figure 3 (bottom) shows the log-weighted comparison of PhotonAssay™ against the CRM values with a mean ratio of  $1.01 \pm 0.01$ , indicating that PhotonAssay™ and fire assay can be used interchangeably on a diverse range of pulverised material types and matrices.

Of the 94 CRMs, five reported mean PhotonAssay™ grades that differed from certified values by more than 2 standard deviations, and only two (CDN-GS-13A at 13.2 ppm and G312-5 at 1.6 ppm) exceeded 3 standard deviations, a result consistent with normal statistical expectation for a dataset of this size and indicative of no systematic bias.

Overall, these results demonstrate excellent consistency between fire assay and PhotonAssay™ and indicate that the two techniques can be used interchangeably across a wide range of sample types.

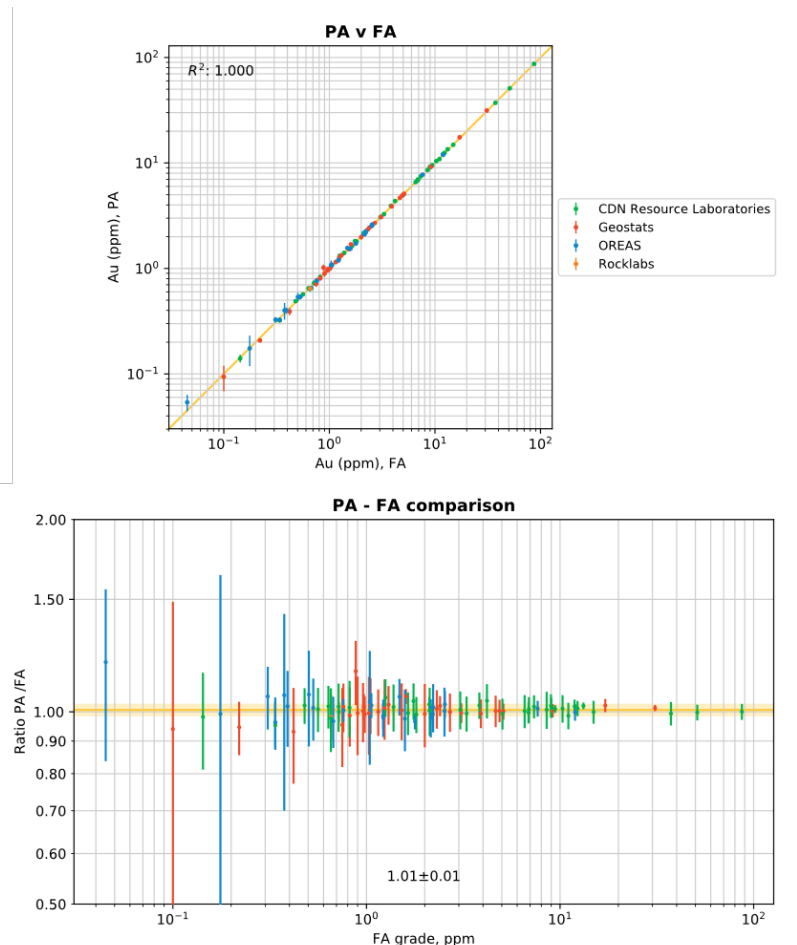


**Figure 3: Top: Comparison of PhotonAssay™ gold grades (y-axis) and certified reference grade (x-axis) for 94 CRMs measured using the PhotonAssay™ system operating in Perth, Western Australia. Bottom: Tukey mean-ratio plot comparing the grades from PhotonAssay™ and fire-assay for the suite of CRMs. The ratio of the paired grades is plotted as a function of the mean sample grade, determined from the average of the two methods. The yellow band indicates the mean ratio and grade ratio variation ( $\pm 1$  SD) averaged over all samples.**

## **4.2. Large-Scale Ore Studies**

Extensive feasibility studies have now been conducted comparing PhotonAssay™ and fire assay across a wide range of ore types and operational environments.

Collectively, these studies comprise:

- More than 10,000 comparisons generated through over 100 Chrysos-led feasibility studies
- More than 200,000 comparison samples analysed across multiple independently-performed customer feasibility study programs
- Comparisons against multiple conventional analytical methods, including fire assay, screen fire assay, and pulverise-and-leach (PAL), as well as comparisons between crushed and pulverised PhotonAssay™ measurements.

These large-scale validation programs demonstrate broad industry evaluation and adoption of PhotonAssay™ performance across diverse operational and geological settings. Studies have evaluated a broad range of sample types from various operational settings, including diamond drill core, reverse circulation chips, blast hole samples and processing samples. Strong agreement between PhotonAssay™ and fire assay was consistently observed across diverse deposit styles.

Most users routinely analyse crushed ore and therefore commission studies comparing PhotonAssay™ performance on crushed product against fire assay. Here, we summarise results from a subset of 15 studies in which PhotonAssay™ analysis was performed on samples both after crushing and again after pulverisation, and fire assay was subsequently performed on the pulverised end product. For simplicity, we exclude studies that used alternative traditional assay techniques such as PAL, or those for which sufficiently detailed geological classification information was unavailable.

Table 1 presents a comparison of the different analytical methods with study results grouped across four major deposit types. With the constraints described above, this represents only a subset of the broader Chrysos feasibility study database.

**Table 1: Summary of feasibility study results across four geological domains. ‘Crushed’ and ‘Pulverised’ refer to PhotonAssay™ measurements performed on samples after different levels of particle size reduction. ‘Mean ratio’ refers to the average pairwise ratio of grades determined using different analysis methods following the process described in section 3; 1-SD uncertainties on the mean ratio are also reported.**

Deposit Type	N Studies	N Pairs	Comparison	Mean Ratio	Correl (R <sup>2</sup> )
Orogenic	9	839	Crushed v Pulverised	1.00 ± 0.02	0.997
		841	Crushed v Fire Assay	1.00 ± 0.02	0.996
		833	Pulverised v Fire Assay	1.00 ± 0.02	0.998
Intrusion	3	772	Crushed v Pulverised	1.00 ± 0.02	0.995
		752	Crushed v Fire Assay	1.00 ± 0.02	0.995
		751	Pulverised v Fire Assay	0.98 ± 0.02	0.996
Epithermal	2	117	Crushed v Pulverised	1.00 ± 0.02	1.000
		114	Crushed v Fire Assay	0.97 ± 0.02	0.998
		113	Pulverised v Fire Assay	0.98 ± 0.02	0.998
Porphyry	1	100	Crushed v Pulverised	1.01 ± 0.02	0.997
		98	Crushed v Fire Assay	0.99 ± 0.02	0.994
		97	Pulverised v Fire Assay	0.97 ± 0.02	0.996

**Note:** Comparisons include only samples with reported grades above 0.01 ppm Au. Minor differences in the number of comparison pairs occur where one or more analytical methods fall below this reporting threshold for a given sample and are therefore excluded.

Across the four deposit types, excellent agreement between crushed PhotonAssay™, pulverised PhotonAssay™, and fire assay gold results is seen. Mean ratio values are statistically consistent with 1.00, with narrow standard error bounds (± 0.02 1-SD), indicating no statistically significant bias between methods. Correlation between the different measurements is also highly consistent across all comparison pairs and geological domains, ranging from 0.994 and 1.00, indicating comparable dispersion irrespective of particle size.

Table 2 summarises the between aliquot grade variability for PhotonAssay™ measurements performed on crushed or pulverised material, or via fire-assay. Whilst reducing the particle top size is generally helpful, in many contexts PhotonAssay™ on crushed ore produces results with comparable precision at lower cost.

**Table 2: Root-mean square relative standard deviations observed between measurements of aliquots taken from the same original sample; results combine both instrument precision and sampling errors.**

<b>Relative Standard Deviation by Sample Preparation and Deposit Type &gt; 0.01ppm</b>			
<b>Deposit Type</b>	<b>PhotonAssay™ Crushed</b>	<b>PhotonAssay™ Pulverised</b>	<b>Fire Assay</b>
<b>Orogenic</b>	<b>18%</b>	<b>16%</b>	<b>36%</b>
<b>Intrusion</b>	<b>19%</b>	<b>13%</b>	<b>35%</b>
<b>Epithermal</b>	<b>10%</b>	<b>9%</b>	<b>7%</b>
<b>Porphyry</b>	<b>23%</b>	<b>18%</b>	<b>22%</b>

Overall, comparisons with fire assay demonstrate that PhotonAssay™ is robust across a range of geological settings, with no material difference evident among the three comparison combinations.

## **5. Detailed Case Studies**

To expand the discussion, we report on two comparison studies in more detail.

### **5.1. Case Study A: Disseminated Gold Deposit**

The first case study was conducted at an operating gold mine hosted in disseminated mineralisation within a West Africa greenstone belt. The deposit is characterised by fine-grained gold occurring predominately microscopic inclusions within sulphide mineralisation, with grade distribution that is broadly homogeneous at the sample scale. Motivations for the client investigating PhotonAssay™ as an alternative to fire assay included the larger sample mass, reduction in sample preparation and faster turnaround time.

#### **Study Design**

The study comprised 250 samples from a disseminated gold deposit, each with a nominal mass of 1 kg. Each sample was crushed (-3 mm) and split into two jars, with PhotonAssay™ undertaken on each jar. Samples were then recombined, pulverised (P80 -75 µm), and split into three jars, with PhotonAssay™ performed on each jar. One jar was randomly selected for fire assay to extinction, with the remaining two jars set aside. This study design allowed direct comparison of PhotonAssay™ performed on crushed and pulverised materials with fire assay.

#### **Results**

Table 3 summarises the results from each comparison pair. PhotonAssay™ on crushed (-3 mm) material versus pulverised (-75 µm) material has a mean grade ratio of  $0.99 \pm 0.02$ , indicating negligible systematic difference between the two particle sizes and confirming that PhotonAssay™ is insensitive to particle size preparation. Comparison of PhotonAssay™ on crushed material against fire assay has a mean grade ratio of  $1.01 \pm 0.02$ , and PhotonAssay™ pulverised against fire assay has a mean grade ratio of  $1.02 \pm 0.02$ . All three methods produce consistent results, with no meaningful normalization difference between any combination of method or particle size.

**Table 3: Summary of results for case study A**

Comparison	N	Mean Ratio	Correlation (R <sup>2</sup> )
PhotonAssay™ Crushed (-3 mm) vs PhotonAssay™ Pulverised (-75 µm)	264	0.99 ± 0.02	0.998
PhotonAssay™ Crushed (-3 mm) vs Fire Assay	265	1.01 ± 0.02	0.994
PhotonAssay™ Pulverised (-75 µm) vs Fire Assay	264	1.02 ± 0.02	0.996

*Note: Comparisons include only samples with reported grades above 0.01 ppm Au. Minor differences between comparison pairs occur where one or more analytical methods fall below this reporting threshold for a given sample and are therefore excluded*

Figure 4 presents the Tukey ratio plots for all three comparisons. Pointwise grade ratios are centred around unity, with no obvious trend versus mean grade across approximately three orders of magnitude. Except at the very lowest grades (< 0.1 ppm) in the PhotonAssay™ crushed versus pulverised chart, where instrument errors start to become appreciable, the charts indicate strong homoscedasticity across the whole grade range; that is, the variance between measurements is independent of grade. This homoscedasticity reinforces that the agreement between methods is robust. Lower variance, indicated by the width of the yellow bands (which show a ±1 SD range), is observed between the two PhotonAssay™ measurements than between either of the PhotonAssay™ results and fire assay, indicating better overall total precision—combined sampling and measurement error—for the PhotonAssay™ measurements performed on larger-mass samples.

### Operational Implications

Findings from this study demonstrate that PhotonAssay™ delivers equivalent results on both crushed and pulverised materials, representing a significant opportunity to reduce sample preparation costs, streamline laboratory workflows, and reduce total assay turnaround time (TAT).

In any gold mine operation, pulverisation represents a substantial component of sample preparation expenditure, requiring dedicated equipment, consumables, maintenance, and labour. It also carries an increased risk of cross-contamination between samples due to the malleable nature of gold. In a conventional fire assay program, pulverisation is a prerequisite to obtaining a representative sub-aliquot from the larger sample mass. Where PhotonAssay™ is deployed, this step can be eliminated entirely without compromising data quality, as demonstrated by the particle size insensitivity observed across the full grade range in this study. The additional benefit of measuring a larger sample mass at the crushed stage further improves representativity compared to a conventional 50 g fire assay aliquot.

Collectively, these operational advantages demonstrate that PhotonAssay™ represents a technically equivalent and operationally superior alternative to conventional fire assay workflows in disseminated gold settings, delivering reduced preparation costs, improved sample representativity, and faster TAT without compromising data quality.

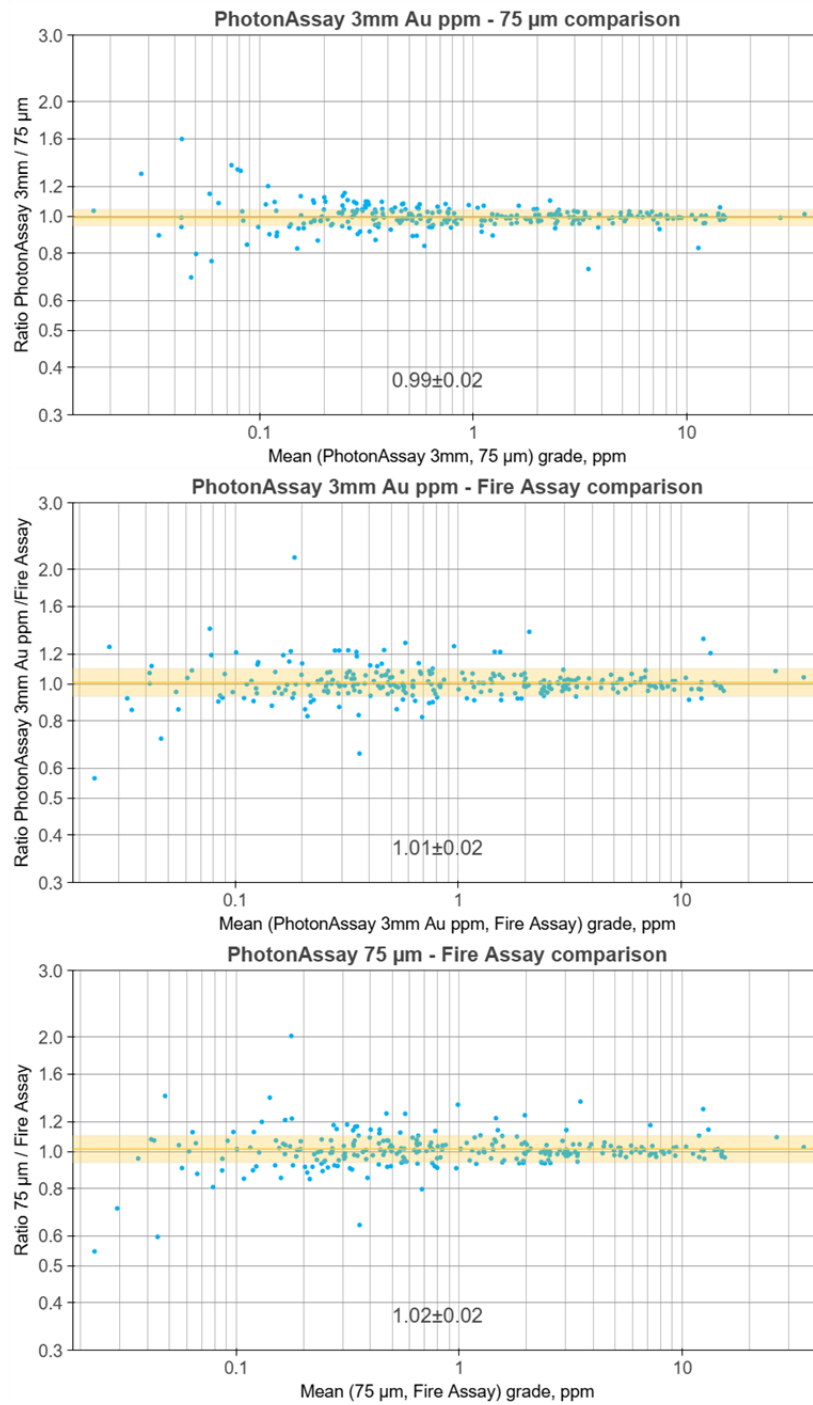


**Figure 4: Tukey ratio plots for all PhotonAssay™ and Fire Assay comparisons for case study A. Blue points represent pairwise grade ratios for individual samples measured using different methods. The gold line shows the log-mean ratio and the yellow band the +/-1 SD width of the grade ratio distribution.**

## 5.2. Case Study B: Coarse Gold Deposit

The second study was conducted at an operating gold mine characterised by coarse, nuggety gold mineralisation. The deposit is structurally controlled, with gold occurring predominantly along shear zones and associated quartz veining, resulting in an inherently heterogeneous gold distribution at the sample scale. This style of mineralisation presents well-documented challenges for representative sampling [17], as the uneven distribution of coarse gold particles introduces significant variability between sub-samples a characteristic that differentiates this setting from the disseminated case study to provide a contrasting framework within which to evaluate PhotonAssay™ performance.

### Study Design

This case study included 150 samples (50 from exploration and 100 run-of-mine), with a nominal mass of 2 kg per sample. Each sample was initially split into two primary halves, with one half retained by the mine (“Original”) for conventional fire assay analysis and the other (“Duplicate”) submitted for PhotonAssay™ investigation. This primary split provided the first comparison point between the two methods.

The PhotonAssay™ Duplicate half was crushed (–3 mm) and split to extinction into typically four jars with PhotonAssay™ undertaken on each jar. Samples were then recombined, pulverised (P80 –75 µm), and jarred to extinction into typically six jars. Additional jars were required to accommodate the volume expansion of the pulverised material. PhotonAssay™ was undertaken on each pulp jar, providing a direct comparison between PhotonAssay™ on crushed and pulverised material. For exploration samples only, the site laboratory performed dual (2 × 50 g) fire assay analysis on the Original split and subsequently provided results to Chryso for an initial comparison.

### Initial Observation – Apparent Bias

Comparison of PhotonAssay™ results on the Duplicate split against the conventional fire assay on the Original split for exploration samples indicated a bias between the two methods. The original fire assay results were biasing 6% higher for crushed material and 8% higher for pulverised material relative to PhotonAssay™ results, as shown in Figure 5. The scatter in the pairwise grade ratios is also significantly larger than what would be expected from analytical errors alone.

### Fire Assay to Extinction

To investigate whether the bias could be attributed to the PhotonAssay™ measurements, follow-up fire assay to extinction was undertaken on every jar, including both the exploration and mining samples. This ensured that all gold present in the Duplicate sample half was captured, eliminating variability associated with sub-sampling error.

Table 4 presents results from several selected high-grade jars of the same sample where fire assay to extinction was performed for each jar, illustrating the degree of variability present between 50 g aliquots that is diagnostic of a persistent nugget effect that pulverisation has not resolved.

Figure 6 presents the mean ratio of PhotonAssay™ and fire assay to extinction results for the whole sample suite. The bias between the PhotonAssay™ and fire assay results is eliminated, and the variance is significantly reduced. Equivalent performance is observed for PhotonAssay™ performed on both crushed and pulverised material. This indicates that the originally observed bias for the exploration samples was associated with splitting the samples into Original and Duplicate halves, or with the subsequent pulverising, sub-sampling, and fire assay analysis undertaken on the Original splits.

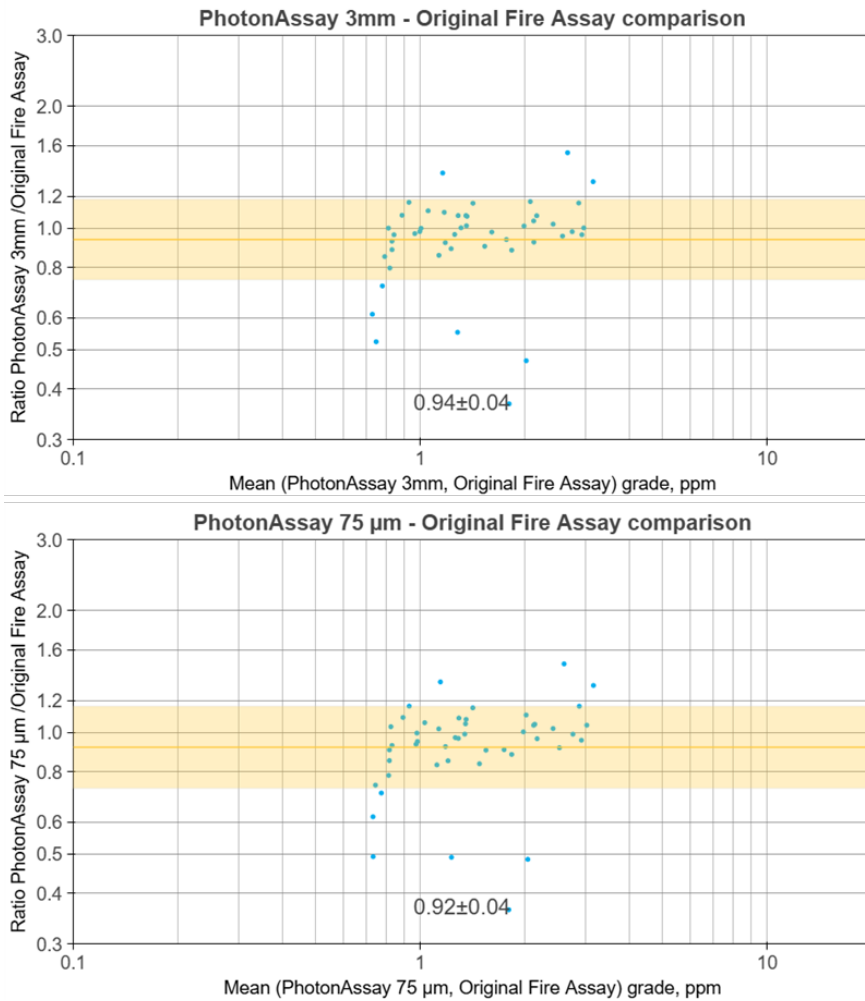
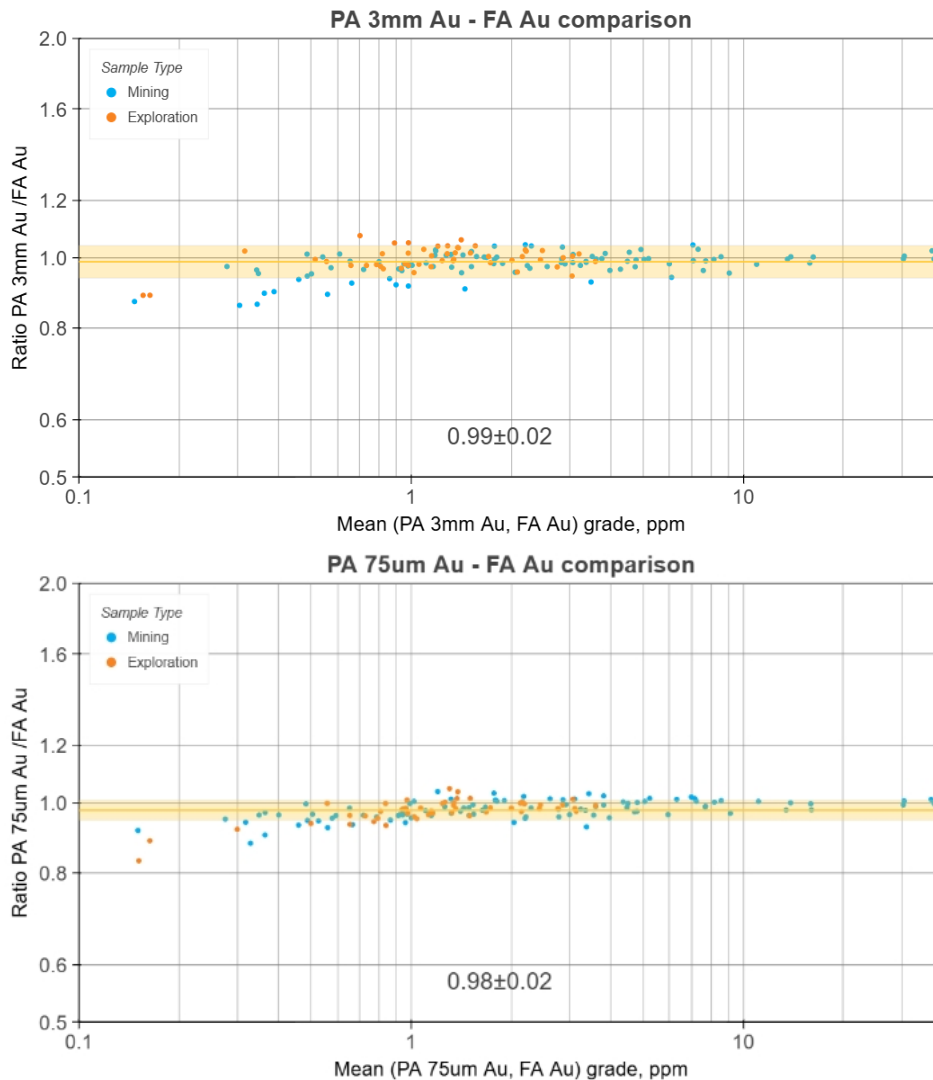


Figure 5: Tukey ratio plots of PhotonAssay™ measurements performed on the Duplicate sample split compared to fire assay measurements on the original split for the 50 exploration samples. See captions to Figure 4 for plot details.

Table 4: Gold grades (ppm) for individual fire assay aliquots performed on 6 PhotonAssay™ jars of pulverised material taken from the same original sample. Whilst individual fire-assay results are highly variable, their average is in excellent agreement with the PhotonAssay™ result measured on the entire jar.

Jar	Fire-assay results (gold, ppm)									PhotonAssay
	Aliquot 1	Aliquot 2	Aliquot 3	Aliquot 4	Aliquot 5	Aliquot 6	Aliquot 7	Aliquot 8	Mean	Gold, ppm Whole jar
A	44.82	36.72	35.14	31.19	35.14	26.36	32.34		34.53	34.80
B	36.49	44.89	33.94	29.72	39.33	35.55	30.84	25.56	34.54	35.36
C	32.95	45.73	40.76	37.57	40.32	37.34	46.51		40.17	38.98
D	49.73	44.47	40.73	32.04	46.70	42.25	38.75		42.10	43.58
E	34.79	40.05	28.67	32.48	29.89	30.38	34.57		32.98	32.64
F	37.74	43.00	45.86	38.12	41.97	43.23	38.59	42.12	41.33	39.76



**Figure 6: Tukey ratio plots comparing PhotonAssay™ and fire assay to extinction results on 50 exploration samples (red points) and mining samples (blue points).**

This case study underlines the importance of follow-up analysis when unexpected results are obtained. In this case, an initial observation of “PhotonAssay™ biases low against fire-assay” was instead resolved as a problem with the original sample splitting or laboratory fire-assay analysis. Further, the fire-assay to extinction work showed the considerable variability between fire-assay aliquots that remained even after pulverization. The ability of PhotonAssay™ to measure an entire 500 g sample is particularly advantageous for such coarse gold deposits, strongly indicating the use of the method.

### Operational Implications

The findings from this case study carry different but equally important operational implications compared to the disseminated deposit study. In a coarse gold system, the nugget effect cannot be resolved through pulverisation alone, as demonstrated by the persistent within-jar variability observed even after reducing material to a 75 µm top size. Conventional fire assay on a 50 g sub-aliquot is therefore an inherently unreliable estimator of true sample grade, regardless of preparation effort applied.

In a coarse gold setting, poor sub-sampling is unforgiving: errors introduced during splitting propagate directly into the assay result and cannot be corrected downstream. It is well recognised [17] that achieving consistent best practice in fire assay sample preparation is operationally difficult, requiring a high level of technical skill, rigorous procedural discipline, and reliable quality oversight at every stage of the preparation process. These demands are

difficult to sustain consistently, particularly at mine sites in remote locations where attracting and retaining skilled laboratory personnel presents an ongoing operational challenge.

PhotonAssay™ offers a meaningful advantage in both respects. Technically, the measurement of the full jar mass reduces the influence of individual coarse gold particles on the result, significantly mitigating the sub-sampling limitation that undermines conventional fire assay in a coarse gold setting. Operationally, the technique requires a comparatively lower level of operator skill to achieve consistent results, reducing dependence on reliable labour and making it more resilient to the workforce variability common in remote mining environments.

## 6. Positional Heterogeneity and Spatial Effects

A central criticism raised in the recent paper by François-Bongarçon and Oliver [16] concerns the positional variations in sensitivity within PhotonAssay™ sample containers, and potential effects on measurement bias. Specifically, they argue that non-uniform spatial distributions of gold, particle segregation, or sample presentation effects may significantly bias PhotonAssay™ measurements.

In this section of our paper, we describe the physics basis of the dependence of sensitivity on position and explore its potential impacts on both bias and measurement precision.

### 6.1. Physical Basis of Spatial Effects

The physics model underlying the operation of PhotonAssay™ was originally published in [6]. A simplified version is presented here.

The basic question to be addressed is straightforward: if a gold atom is located at a particular location inside a PhotonAssay™ jar, what is the probability that it will be activated and its gamma-ray emission subsequently detected?

The detection probability  $p$  is the product of three factors:

$$p = S \cdot D \cdot T \quad (2)$$

The source factor  $S$  relates to the intensity (or flux) of the incident X-rays; the higher the intensity, the more likely a gold atom is to be activated. The X-ray beam from the accelerator is not 'laser-like' but is emitted over a cone with an apex angle of about 20° (the off-axis flux drops to one half of the peak on-axis flux at a half-angle of about 10°). The flux decreases with distance from the source, so with the X-ray beam incident horizontally, it is greater on the side closest to the source.

The detector factor  $D$  captures the probability that the gamma-ray emitted by an activated gold atom will be successfully detected. Detection relies on three things occurring: the gamma-ray being emitted towards a detector (its initial direction is completely random); the gamma-ray escaping from the sample without interacting; and the gamma-ray depositing all its energy in the sensitivity volume of the detector. Practically, the closer a gold atom is positioned with respect to a detector, the higher the chance of its emission gamma-ray being recorded, as the detector subtends a larger solid angle at the decay position, and there is less intervening material to absorb the gamma-ray before it exits the sample.

Last and most straightforward is the time factor  $T$ . This captures the time-dependent aspects of the detection process, namely the increasing probability of a gold atom being activated the longer it is exposed to the X-ray beam, offset by the chance that it can randomly decay before reaching the detector system. Similarly, the longer the sample spends in the detector, the greater the chance that the atom decays can be detected. The time factor  $T$  does not depend on the position of gold atom within the sample, so does not need to be considered further in this discussion.

## 6.2. Mitigation of Spatial Effects through System Design

The variation in the source and detector factors with position can be mitigated through careful design of the activation and measurement systems.

Key mitigation factors include:

- Rotation of the sample during activation at a speed significantly faster than the gold activation half-life. The 60-rpm rotation speed (one revolution per second) substantially eliminates the 'hot-spot' on the side of the jar closest to the accelerator.
- Positioning two detectors above and below the sample and combining their results significantly equalises the detection response.
- Using large-diameter detectors that approximately match the diameter of the sample jars. The 100 mm diameter of the PhotonAssay™ sample jars was chosen with reference to a 90 mm detector diameter, the largest readily available commercially.
- Carefully selecting the disposition of the sample jar with respect to both the accelerator and detectors to compensate for remaining variations in  $S$  and  $D$  with position.

In arriving at a final design, positional effects must be balanced against sensitivity and sample size. For example, using a much smaller sample jar would reduce positional effects, but significantly decrease sensitivity and increase the Fundamental Sampling Error.

The total measurement variance  $\sigma_T$  can be written as:

$$(3) \quad \sigma_T^2 = \sigma_{\text{sampling}}^2 + \sigma_{\text{positional}}^2 + \sigma_{\text{measurement}}^2$$

where the three terms on the right capture contributions from the Fundamental Sampling Error, positional sensitivity and measurement precision respectively. The variances due to sampling and measurement decrease proportional to sample mass, whereas the positional variance increases with jar size (and hence sample mass). The PhotonAssay™ jar size of 320 mL was chosen to optimise the total measurement variance.

Optimising the design of a PhotonAssay™ system to minimise the total measurement variance is a complex problem, as it depends in detail on the physics of X-ray emission, gamma-ray production, scattering and attenuation inside the sample, and detector operation. Computer Monte Carlo modelling methods [18] were extensively used to allow large numbers of design variations to be simulated and their performances compared. Careful experimental validation was then required to confirm the modelled designs.

## 6.3. Magnitude of Spatial Effects

François-Bongarçon and Oliver [16] present results of an experiment to measure the positional sensitivity variations of a PhotonAssay™ unit. They tabulate the average grade reported from 5 measurements of a gold particle positioned at different locations inside a sample jar. These results are in agreement with simulated results which were reported in Chryso technical note TN-121 and are shown in Figure 7.

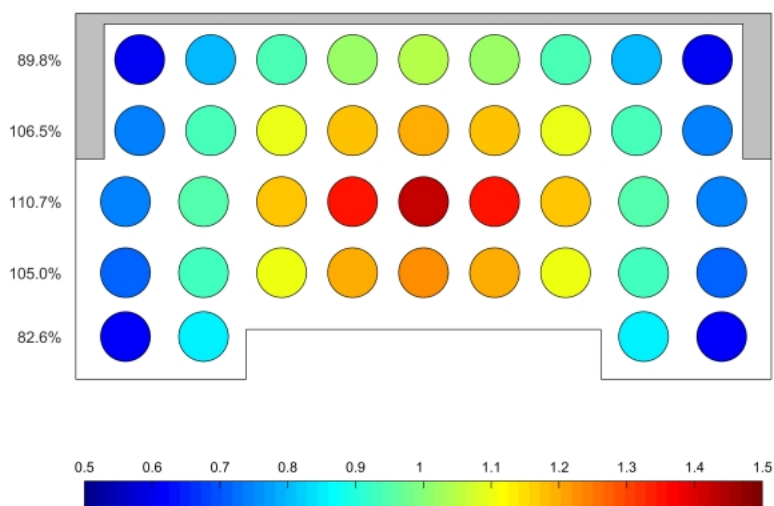


**Figure 7. Sensitivity for a gold particle located at different locations throughout a section of a PhotonAssay™ sample jar. The values on the left are the weighted average sensitivities versus vertical position. See text for details.**

The coloured circles in Figure 7 indicate the grade that would be reported if all the gold in a sample were present at that location, divided by the grade that would be reported if the same amount of gold was uniformly distributed throughout the sample volume. The numbers on the left show the relative sensitivity of horizontal ‘layers’ of material inside the jar. Figure 7 illustrates a section passing through the centre of the jar.

The greatest variations in sensitivity are radial, with strongest gold detection occurring close to the jar axis and weakest detection near the jar outer walls. The standard deviation in sensitivity for a randomly located gold particle is 32% - this indicates the relative standard deviation (RSD) of gold results that would be expected for repeat measurements of a jar containing a single gold particle where the particle is relocated at complete random between runs. The vertical sensitivity is significantly less, approximately ±12-17%.

### 6.4. Practical Significance

The practical significance of spatial effects on PhotonAssay™ performance can be explored with reference to both precision and bias.

Consider precision first. The total analytical variance (Figure 8) is the sum of the variances arising from the Fundamental Sampling Error, positional effects and measurement precision. This represents the variance that would be observed between measurements performed on different sample aliquots drawn from an original bulk lot. The sum of the positional and measurement variances represents the variance that would result from performing repeat measurements on the same sample, with sufficient mixing between runs to completely randomise the location of any gold nuggets. Last, the measurement variance alone corresponds to multiple repeat measurements of the same sample performed without any mixing or internal movement.

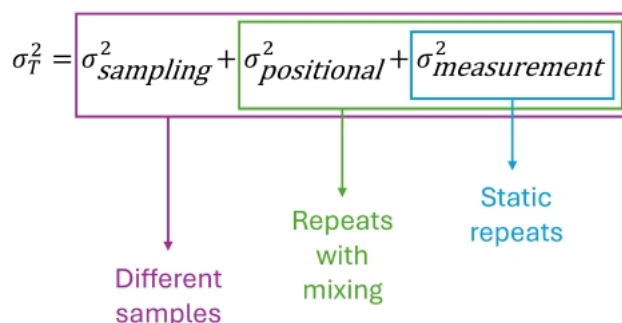


## Figure 8. Contributions to total analytical variance and physical interpretation.

The Fundamental Sampling Error ( $\sigma_{\text{SAMPLING}}$ ) is given simply by  $1/\sqrt{N_{\text{EFF}}}$  where  $N$  is the number of gold particles or nuggets in the sample,  $N_{\text{EFF}} = N/(1 + CV_{\text{NUG}}^2)$  is an effective number of nuggets which is smaller than  $N$  due to the breadth of the nugget mass distribution, and  $CV_{\text{NUG}}$  is the coefficient of variation (relative SD) of the nugget mass distribution. For the case of a sample where the expected number of contained gold nuggets is one, the FSE is 100%.

The positional sensitivity effect is approximately 32% (1-SD) for a single gold nugget measured for a single cycle, or 23% for a standard 2-cycle measurement<sup>1</sup>. For a sample whose gold content is divided between multiple nuggets, the positional effect is reduced, assuming that the positions of the different nuggets within the jar are uncorrelated. The positional error is then  $k/\sqrt{N_{\text{EFF}}}$  where  $k = 0.23 - 0.32$  depending on the degree of mixing that occurs between cycles.

Finally, the measurement error arises mainly from statistical fluctuations in the number of observed gold decay gamma-rays; this is well understood and reported sample-by-sample. The 1-SD precision varies from about 12% at 0.1 ppm, 6.5% at 0.3 ppm gold content, 4% at 1 ppm to 2.5 % at 3 ppm and to < 2% at gold grades above 10 ppm.

We can now investigate the impact of combining these different sources of uncertainty for some cases of interest.

*Repeat measurements with mixing.* For coarse gold samples with a grade of 1 ppm or over containing relatively few nuggets in a 500 g aliquot (say  $N_{\text{EFF}} < 100$ ), repeat measurements will vary by more than the reported instrument precision. In very coarse materials (say  $N_{\text{EFF}} < 10$ ), the RSD between repeats may be 10-30%, an order of magnitude greater than the underlying instrument precision. Samples that exhibit significantly different results in the top or bottom detectors, or between measurement cycles are automatically flagged 'HET' by the PhotonAssay™ reporting system.

*Measurements on separate aliquots.* The sum of the FSE and positional sensitivity contribution is given by  $\sqrt{\sigma_{\text{sampling}}^2 + \sigma_{\text{positional}}^2} = \sqrt{(1 + k^2)/N_{\text{EFF}}} = \text{FSE} \cdot \sqrt{(1 + k^2)}$ . In other words, the effect of positional sensitivity is to increase the FSE by a factor of  $\sqrt{(1 + k^2)} = 1.025 - 1.05$ . Equivalently, positional sensitivity reduces the effective sample mass by a factor of 2.5-5%, meaning that a 500 g sample is reduced to a 475-490 g mass from a perspective of total measurement uncertainty. This is a small effect.

Consequently, we arrive at the conclusion that whilst positional effects can produce large increases in measurement uncertainty for repeat tests performed on the same sample, their impact on overall measurement uncertainty (including the Fundamental Sampling Error) is marginal. The samples where large positional effects are seen – those containing a small number of gold particles – are precisely those where sampling errors are largest.

Next, let us consider the impact of positional effects on bias. We use the term 'bias' to refer to a systematic under or over-reporting of grade, either for repeat measurements of an individual sample (with complete mixing between assays), or for a large suite of separate samples. Variations in reported grade for individual measurements are captured in the variance discussions above.

By construction, if locations of gold nuggets within the sample volume are truly uniform (meaning that all positions are equally likely to occur), then no bias is present. This is because the calibration of a PhotonAssay™ instrument is derived experimentally from

---

<sup>1</sup> Assuming that the nugget location randomly changes between measurement cycles; this represents experimentally observed behaviour in samples that are not packed too tightly to prevent movement.

measurements performed on uniform materials (generally certified reference materials or similar). If gold nuggets in a non-uniform material report randomly to any location, then on average their grade will correspond to the same grade that would be reported if the small mass of gold were uniformly distributed throughout the jar volume.

For a bias to arise, it is therefore necessary for gold particles to systematically report to certain locations more often than others. With reference to Figure 7, if gold particles preferentially report to the outer surface of the jar, for example, such samples would underread compared to samples containing the same amount of gold where particles report to the central axis of the jar.

We consider the most likely form of bias to be caused by vertical segregation, where owing to density, hardness or particle size effects, gold-bearing ore particles are preferentially sorted towards either the top or bottom of the sample. We have modelled the system response for five simulated scenarios:

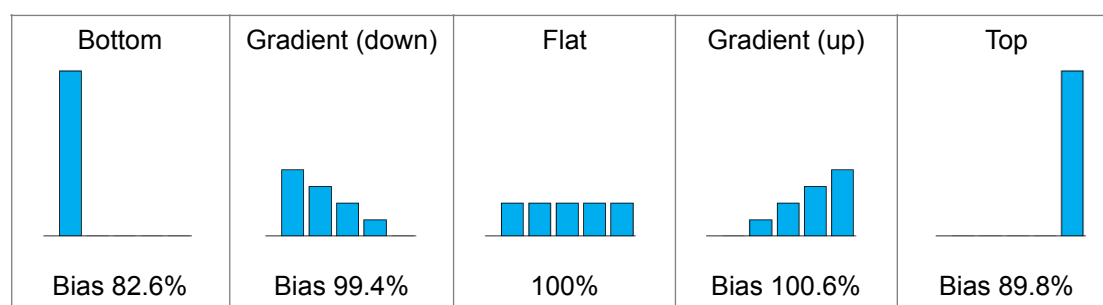
- 'Bottom' – all gold is present in the bottom 10 mm layer of material in the jar
- 'Gradient (down)' – the density of gold particles decreases linearly from a maximum at the bottom of the jar to zero at the top of the jar
- 'Flat' – gold particles are uniformly distributed throughout the jar
- 'Gradient (up)' – the reverse of 'Gradient (down)'
- 'Top' – all gold is present in the top 10 mm layer of material in the jar.

Results on the overall system response for these five scenarios are summarised in Figure 9. The response for the flat distribution is normalised to 100%.

For the two 'Gradient' cases, the variation in gold sensitivity is below 1%. This is because the variation in gold sensitivity versus height inside the jar is approximately symmetric about the jar centre. 'Missing' gold near the top of the jar is offset by additional gold near the bottom of the jar and vice versa, resulting in little change in overall sensitivity. Only in the extreme cases where all gold is present in the low sensitivity regions at the very top or bottom of the jar is there a significant drop-off in response, amounting to 10-17%.

In cases of significant segregation, the gold signals received by the detectors positioned above and below the sample during measurement will be discordant. For example, in the 'Bottom' case the signal in the detector below the sample is approximately 5 times as large as the signal in the detector above the sample, with the converse result for the 'Top' case. Samples flagging such disagreement between the two detectors are automatically flagged 'HET' in the batch report. Manual review of the results from the two detectors can provide further indication of systematic gold segregation if required.

**Figure 9. System responses for gold relative to uniform case ('Flat') for different distributions of gold particles within a full jar of ore. The bar charts indicate the relative proportions of gold present in 5 × 10 mm thick layers arranged from the bottom to the top of the jar.**



How common are these different scenarios in practice? The evidence presented in sections 4-5 suggest that the extreme 'top' and 'bottom' scenarios do not generally occur, as they would result in significant, systematic low biases in measured gold grades. Extreme top/bottom detector calculated gold grades are also not observed.

Repeat measurements on sample suites are commonly performed on PhotonAssay™ units located on different sites, typically as part of inter-lab round robins during early-stage feasibility studies, or as part of routine quality assurance by larger PhotonAssay™ users. Systematic shifts in grade, which would indicate potential material segregation during transport, are not observed.

Significant vertical segregation would also be indicative of severe issues with sample preparation and splitting. If the preparation of a PhotonAssay™ aliquot results in the majority of the gold reporting to either the top or bottom of the jar, this would suggest that gold is not evenly distributed during the splitting process; the splitting itself may then be introducing a bias.

## 7. Discussion and Conclusions

PhotonAssay™ is designed to provide robust analysis of gold in a wide range of materials. The well-understood physics of isomer activation, decay and measurement allow accurate models to be constructed to predict analysis performance, including instrument precision, detection limit, particle size and material composition effects, and sensitivity to sample heterogeneity.

Accumulated evidence from extensive testing on certified reference materials, inter-laboratory round-robins, large-scale validation and feasibility studies and operational experience running to tens of millions of samples has validated these models and demonstrated that PhotonAssay™ provides robust measurements of gold grade across a broad range of ore types.

The principal observations emerging from these studies are:

- PhotonAssay™ measurements on crushed and pulverised materials are self-consistent.
- PhotonAssay™ exhibits strong agreement with established analytical techniques across diverse deposit types
- Larger assay masses frequently reduce total sampling variance relative to small-charge fire assay, even on crushed material
- Observed discrepancies between methods are often dominated by ordinary sampling effects rather than instrumental bias
- Spatial heterogeneity effects exist but are modest in practical operational contexts

- Appropriate choice of comparison methodology is essential when evaluating assay method equivalence, particularly for highly heterogeneous ores.

Where statistically significant biases are seen, whether between PhotonAssay™ measurements performed on different material preparations (crushed versus pulverised, for example) or between PhotonAssay™ and traditional methods, a rigorous evaluation should be performed. Our experience from more than 100 comparison studies indicates that differences can usually be attributed to one or more of the following factors:

- Inappropriate statistical treatment of the data, such as poor choice of bias estimator, handling of below detection limit (BDL) samples, sample swaps etc
- Contamination, particularly during the pulverisation step, leading to transfer of gold from high grade to low grade samples
- Poor splitting practices
- Unaccounted-for losses or normalisation uncertainty in the comparison method, for example incomplete gold recovery during fire assay or leach analysis
- Inaccurate measurement of fill levels of PhotonAssay™ jars, particularly for pulverised materials, where recommended fill procedures have not been followed.

Spatial response variations and positional heterogeneity effects are physically real phenomena and can be understood appropriately within the framework of radiation transport and sampling theory. However, a theoretical analysis and extensive experimental evidence indicates that these effects are generally small compared with the broader sources of variability inherent in gold ore sampling and assay workflows.

PhotonAssay™ represents a fundamentally different approach to gold analysis, based on direct non-destructive bulk measurement rather than chemical extraction from small aliquots. Notwithstanding its widespread use and industry acceptance, as with any assay method it is important to continue to compare its performance with existing techniques and understand any systematic differences.

The Chrysos team has extensive experience in conducting and evaluating comparison trials and are happy to provide advice or assistance.

## 8. References

[1] Hoffman, E.L., Clark, J.R., Yeager, J.R., 1999. Gold analysis – fire assaying and alternative methods. *Explor. Min. Geol.* 7 (1+2), p. 155–160.

[2] Otvos, J., Guinn, V., Lukens, J., Wagner, C., 1961. Photoactivation and photoneutron activation analysis. *Nucl. Instr. and Meth.* 11, p. 187–195.

[3] Glukhikh, V.A., Muntyan, V.I., Burmistenko, Y.N., Ivanov, I.N., Feokistov, Y.V., Shtan, A.S., 1979 Industrial gamma activation laboratory analysis of ore samples for gold and interfering elements, In: *All-Union Conference on Using Charged Particles Accelerators in National Economy [sic]*. Leningrad, USSR, p. 131.

[4] Burmistenko, Yu.N., 1981. Gamma activation installation for fast determination of gold and its accompanying elements in ore sample. *Isotopenpraxis* 17 (6), p. 241–243.

[5] Řanda, Z., Špaček, B., Mizera, J., 2007. Fast determination of gold in large mass samples of gold ores by photoexcitation reactions using 10 MeV bremsstrahlung. *J. Radioanal. Nucl. Chem.* 271 (3), p. 603–606.

[6] Tickner, J, Ganly, B, Lovric, B and O'Dwyer, J, 2017. Improving the sensitivity and accuracy of gamma activation analysis for the rapid determination of gold in mineral ores. *Applied Radiation and Isotopes*, 122, p. 28-36.

[7] Treasure, D and Tickner, J, 2019. Gold analysis using PhotonAssay: deployment and operating experience, in *Proceedings World Gold 2019*, pp 235243 (The Australasian Institute

of Mining and Metallurgy: Melbourne)

[8] Tremblay, C., Wheeler, G. and Oteri, A, 2019. PhotonAssay™ – Efficient & bulk gold analysis in the modern world, ASEG Extended Abstracts, Volume 2019, Issue 2nd Australasian Exploration Geoscience Conference: Data to Discovery, Dec 2019, p. 1 – 4

[9] Dominy, S, Graham, J, Esbensen, K and Purevgerel, S, 2024. Application of PhotonAssay™ to coarse-gold mineralisation – the importance of rig to Assay optimisation. Sampling Science and Technology 2024 (1) p. 1-30

[10] Chrysos Corporation, 2018. TN-101 PhotonAssay™ Measurement Performance for Gold in Ore Samples. Chrysos Technical Note, available on request from corresponding author.

[11] Huang, X and Zhou, C, 2005. Nuclear Data Sheets for A = 197. Nuclear Data Sheets 104 (2) p. 283-426.

[12] Gy, P, 1973. The Sampling of Broken Ores – A Review of Principles and Practice. Geological, Mining and Metallurgical Sampling, p. 194–205

[13] Chrysos Corporation, 2019. TN-001 Chrysos PhotonAssay™ measurement performance for Gold on Certified Reference Materials. Chrysos Technical Note, available on request from corresponding author.

[14] Chrysos Corporation, 2022. TN-003 Chrysos PhotonAssay™ measurement performance for precision gold services. Chrysos Technical Note, available on request from corresponding author.

[15] Tickner, J, Lannan, O and Preston, R, 2021. Comparing different assay methods for the determination of mineral ore grade. Journal of Geochemical Exploration 226(3-4), p.106780.

[16] François-Bongarçon, D and Oliver, R, 2026. Photon Assaying: a New, Revolutionary Technique Everyone Wants to see Succeed. Sampling Science and Technology 2026 (in preparation).

[17] Dominy, S.C. and Xie, Y. 2016. Optimising sampling protocols via the heterogeneity test: challenges in coarse gold mineralisation. Tr. of the Inst. of Mining and Metallurgy, Mining Technology, 125, p. 103–113.

[18] Bencardino, R, Roach, G, Tickner, J and Uher, J 2010. Efficient Monte Carlo simulation of delayed activation analysis experiments. Nucl. Instr. Meth. In Phys. Research Sec B, 268 (5) p. 513-518.